Journal of Peptide Science
J. Pept. Sci. 2008; **14**: 1022–1031
Published online 9 May 2008 in Wiley InterScience (www.interscience.wiley.com). DOI: 10.1002/psc.1038

JOURNAL OF PEPTIDE SCIENCE

Targeting the c-Myc coiled coil with interfering peptides

EVA M. JOUAUX, KARIN SCHMIDTKUNZ, KRISTIAN M. MÜLLER and KATJA M. ARNDT*

Institute for Biology III, Albert-Ludwigs University of Freiburg, Schaenzlestr. 1, D-79104 Freiburg, Germany

Received 20 November 2007; Revised 22 January 2008; Accepted 27 February 2008

Abstract: c-Myc is one of the most frequently deregulated oncogenes in human cancers, and recent studies showed that even brief inactivation of Myc can be sufficient to induce tumor regression or loss. Consequently, inactivation of Myc provides a novel therapeutic opportunity and challenge, as the dimerization of Myc with Max is crucial for its function. We applied two strategies to specifically target this coiled coil mediated interaction with interfering peptides: a dominant-negative human Max sequence (Max) and a peptide selected from a genetic library (Mip). Both peptides form coiled coils and were fused to an acidic extension interacting with the basic DNA-binding region of human Myc. The genetic library was obtained by semi-rational design randomizing residues important for interaction, and selection was carried out using a protein-fragment complementation assay. The peptides Max and Mip easily outcompeted the human Myc : Max interaction and successfully interfered with the DNA binding of the complex. Both interfering peptides exhibited higher T_m ($\Delta T_m = 13$ and 15 °C) upon interaction with Myc compared to wt Max. The inhibitory effect of the two interfering peptides on human Myc : Max activity makes them promising molecules for analytical and therapeutic Myc-directed research. Copyright © 2008 European Peptide Society and John Wiley & Sons, Ltd.

Keywords: Myc; Max; coiled coil; leucine zipper; rational design; library selection; dominant-negative; protein-fragment complementation assay

INTRODUCTION

Myc has been shown to be involved in cell proliferation, apoptosis, metabolism and differentiation. Furthermore, it is also one of the most frequently deregulated oncogenes in human cancers, often associated with aggressive tumors, including breast, colon, cervical, small-cell lung carcinomas, osteosarcomas, glioblastomas, melanomas and myeloid leukemias [1,2]. Recent studies showed that in some cancers brief inactivation of Myc is sufficient to induce tumor regression, sometimes even leading to tumor loss [3–5]. In other cases, inactivation of Myc induces a state of tumor dormancy and upon Myc reactivation, tumors rapidly reoccur [6–8]. Collectively, these results demonstrate that targeted inactivation of Myc provides a novel therapeutic opportunity and challenge. Low molecular weight inhibitors that prevent Myc : Max heterodimerization have already been discovered [9–11], but the nature of the interaction has not been reported. Some of them are not specific as they also inhibit Jun [10]. Only recently, two small molecules were described that preferentially inhibited DNA binding of Myc : Max over other related dimeric transcription factors [11]. They were able to inhibit c-Myc dependent cell proliferation, gene transcription, and oncogenic transformation in the low micromolecular range. D'Agnano *et al.* described short peptides, based on the Max Zip sequence, that impaired transcriptional activity of Myc *in vivo* [9]. However, none of these studies [9–11] described any thermodynamic analysis of the interaction stability.

c-Myc is the widely studied cellular homologue of the viral oncoprotein (v-Myc) of the avian myelocytomatosis retrovirus [12]. Myc is a bHLHZip transcription factor which belongs to the Myc-Max-Mxd (the last is also known as Mad) transcription network [13]. Myc has an *N*-terminal transcriptional activation domain (TAD) followed by a basic-helix-loop-helix-leucine zipper (bHLHZip) motif, consisting of two α-helices separated by a loop [14]. The first helix is composed of the basic, DNA-binding region and of helix 1 of the helix-loop-helix (HLH) motif; the second α-helix includes helix 2 of the HLH motif and the Zip. The specificity of dimerization is solely mediated by the Zip [15]. Consequently, this provides an attractive target for the development of Myc-specific inhibitors. Zip's are a subclass of dimeric parallel coiled coils characterized by a predominance of leucine at every seventh position (position *d*) of the heptad repeat (denoted a-g) [16–19]. The coiled coil is widespread in nature; it is estimated that approximately 3–5% of all amino acids encoded in proteins form a coiled coil structure [20]. The hydrophobic core at the interhelical interface is formed by residues of positions *a* and *d* [21]. Positions *e* and *g* form the edge of the interface and often contain charged or polar residues, which are generally placed to be complementary, allowing for beneficial interhelical salt bridges in a $g_i \rightarrow e'_{i+1}$ manner (where g_i denotes the *g* position of one heptad and e'_{i+1} the *e* position of the following heptad of

Abbreviations: bHLHZip, basic-helix-loop-helix-leucine zipper; CD, circular dichroism; DHFR, dihydrofolate reductase; Mip, Myc-interfering peptide; PCA, protein-fragment complementation assay; TAD, transcriptional activation domain.

*Correspondence to: Katja M. Arndt, Institute of Biology III, Albert-Ludwigs University of Freiburg, Schaenzlestr. 1, D-79104 Freiburg, Germany; e-mail: Katja@biologie.uni-freiburg.de

the other strand). They add to the stability of the dimer and can also aid in heterospecificity by disfavoring homotypic interactions ([22,23] and references therein). Positions *b*, *c*, and *f* are solvent-exposed, mostly polar residues that enhance protein solubility. These three positions have been shown to be variable within the protein sequence. They may also further stabilize the coiled coil by, e.g. intrachain electrostatic interactions or interaction with the helix macrodipol [24].

Transcriptional regulation and oncogenic transformation by Myc requires its heterodimerization with Max and binding to E-Box DNA sequences with the core consensus sequence CACGTG [25]. It has been shown that c-Myc homodimerizes very poorly. All newly synthesized c-Myc are found in complex with Max, indicating that c-Myc preferentially forms a heterodimeric complex with Max which is needed for proper function [26–28]. The homodimerization of the c-Myc protein is prevented by two E residues at core *a* positions (*a*2, *a*3) in the Zip (Figure 1) [29,30], and in fact, all proteins known to date that interact with Max have a conserved acidic residue (either E or D) in the dimerization interface. The NMR solution structure of the DNA binding c-Myc : Max heterodimer showed that the electrostatic interactions between these two E side chains (*a*2, *a*3) in the c-Myc Zip and the H side chain (*d*2) in the Max Zip are responsible for the specificity of heterodimer formation [31]. Nair *et al.* crystallized the Myc : Max complex bound to DNA and found that the tetrad $R_{g3,Myc}$-$R_{a4,Myc}$-$Q_{g3,Max}$-$N_{a4,Max}$ is crucial for directing interaction stability and specificity of Myc and Max [28]. Other studies had shown that both, the Zip and the HLH region, are required for the formation of a stable c-Myc : Max heterodimer [27,32].

Oncogenic activation of myc genes occurs mainly through deregulated expression that leads to a shift of the equilibrium in the Myc-Max-Mxd network towards Myc : Max complexes [33]. Consequently, peptides interfering with Myc : Max dimerization by sequestering c-Myc may open a way for regulating oncogenic Myc. Here, we report the targeting of the human Myc Zip with interfering peptides generated using two strategies. First, we created a dominant-negative human Max by the substitution of the DNA-binding region with an acidic extension to prevent DNA binding. Second, we combined rational design with *in vivo* selection to identify inhibitory peptides replacing the Max sequence. For the second approach, a genetic library was generated with design strategies focusing on maximizing charge attraction, while minimizing repulsion and steric hindrance in the heterodimer. Identification of the best interacting pairs was performed using an *in vivo* PCA combined with growth competition [24,34,35]. In this PCA, cell survival is coupled to the complementation of two fragments of the murine DHFR (mDHFR) linked to either Myc or a library member. Only coiled coil mediated interaction between Myc and a library member generates functional enzyme, and hence leads to cell survival. By fusing an acidic extension [36] to the PCA-selected Mip as well as to the human wt Max HLHZip sequence, we show that these inhibitors can successfully outcompete human Myc : Max interaction and, more importantly, interfere with DNA binding of the human Myc : Max complex. Such inhibitors are promising tools for dissecting the molecular role of Myc in tumorigenesis.

MATERIALS AND METHODS

Library Construction and Cloning

The DNA constructs encoding the *N*-terminal (amino acids 1–107) and *C*-terminal (amino acids 108–186) fragment of the mDHFR fragments have been cloned according to Pelletier *et al.* [35,37] in pQE16 (Qiagen). *Spe*I and *Hind*III restriction sites were added to flank the DHFR sequences. Each plasmid encodes a His_6-tag, *Nhe*I and *Asc*I restriction sites for cloning of the coiled coil sequence, and a short, flexible linker in 5′ position of the DHFR-fragments (Jouaux, Willemsen and Arndt, unpublished data). Mega-primers, flanked by the *Nhe*I and *Asc*I sites, were synthesized including relevant degenerate codons in the case of the library. A fill-in reaction resulted in 111-bp double-stranded oligonucleotides, which were cloned in the respective DHFR vectors, resulting in pAR300d-Myc-DHFR1 (Chloramphenicol resistance, Cm^R), pAR200d-Max-DHFR2 (Ampicillin resistance, Amp^R), and the library containing plasmid pAR200d-Lib-DHFR2 (Amp^R). The plasmid was electroporated into BL21 gold cells (Stratagene) containing the target plasmid and pREP4 (Qiagen; encoding the lac repressor).

In order to verify that the library populations encoded the designed amino acids with the expected frequency, single clones from the library were randomly picked and sequenced. No statistically significant bias was detected. The library was two-fold overrepresented.

DHFR-Assay

The DHFR PCA has been described in more detail elsewhere [35]. Briefly, in the single step selection, selective pressure for the mDHFR was maintained throughout all steps by inhibiting the bacterial DHFR with trimethoprim (1 μg/ml) in M9 minimal medium. Ampicillin (Amp, 100 μg/ml), Chloramphenicol (Cm, 25 μg/ml) and Kanamycin (Kan, 50 μg/ml) were also included in all steps to retain the library plasmid (Amp^R), the plasmid encoding the Myc helix (Cm^R) and the plasmid encoding the lac repressor (Kan^R). Expression of the proteins was induced with 1 mM IPTG. For selection on solid medium, growth was allowed for 67–96 h at 37 °C in BL21 cells. For the competition selection, pooled cells from solid medium were propagated through 10 rounds of selection in liquid M9 medium under selective conditions (described above). For the selection, the starting OD_{600} was 0.0001 in 100 ml medium. Cultures were incubated at 37 °C until an OD_{600} of 0.2 to 1.0 was reached. The culture was directly used to inoculate the next passage as described in [35]. To assess selection progress, individual clones as well as DNA from pooled rounds were sequenced.

DOI: 10.1002/psc

Protein Sequence, Expression and Purification

Human bMyc and bMax variants consist of the basic DNA-binding region (underlined), the HLH region and the Zip domain (bold) followed by a hexa-histidine tag (bMyc: NVKRRTHNVLERQRRNELKRSFFALRDQLPELENNEKAPKVVI LKKATAYILS**VQAEEQKLISEEDLLRKRREQLKHKLEQL**GA PHHHHHH; bMax: ADKRAHHNALERKRRDHIKDSFHSLRDS VPSLQGEKASRAQILDKATEYIQY**MRRKNHTHQQDIDDLKR QNALLEQQVRAL**GAPHHHHHH). In aMax, the basic region of bMax (underlined) is replaced with an acidic extension (PDEEEDDEEELEELED) [36]. aMip differs from aMax in the Zip region by the residues indicated in Figure 1.

Genes coding for the proteins of interest fused to a *C*-terminal His_6-tag were synthesized and inserted into pQE-16 (Qiagen) vector derivatives via *Sph*I and *Hind*III sites, resulting in the vectors pAR300d-bHLHMyc, pAR300d-bHLHMax, pAR200d-aHLHMip, and pAR200d-aHLHMax. Protein expression was performed in *E. coli* BL21 with pRep4 (Qiagen) at 30 °C in 2YT medium for 7–8 h. Cells were induced with 1 mM IPTG after 1.5 h and grown for 6 h before harvesting.

His_6-tagged proteins were purified with a self-packed NiNTA column containing 1 ml of NiNTA superflow (Qiagen). The expression culture pellet was resuspended in 20 ml binding buffer (50 mM sodium phosphate, 150 mM NaCl, pH 7.2), sonified and centrifuged. The steril-filtered (0.45 μm) supernatant was loaded manually with a syringe. Purification of bMax and aMip was performed using a step gradient starting with washing, using 5 column volume (CV) binding buffer and 5 CV wash buffer (50 mM sodium phosphate, 300 mM NaCl, 20 mM imidazol, pH 7.2). Elution of proteins was performed with 4 ml elution buffer (50 mM sodium phosphate, 300 mM NaCl, 250 mM imidazol, pH 7.2). For the purification of bMyc, denaturing conditions were chosen because of low yields with the native procedure. The pellet was resuspended in denaturing binding buffer (100 mM NaH_2PO_4, 10 mM Tris base, 8 M urea, pH 8.0). The protein was refolded on the column: 4 CV denaturing binding buffer, 4 CV denaturing wash buffer (100 mM NaH_2PO_4, 10 mM Tris base, 8 M urea, pH 6.3), 4 CV 1 : 1 mixture of denaturing wash buffer and binding buffer, 4 CV binding buffer. Elution of the protein was performed with 4 ml elution buffer.

Proteins obtained from NiNTA purification were further purified by reverse-phase HPLC using a Jupiter Proteo column (4 μm particle size, 90 Å pore size, 250 × 10 mm; Phenomenex). The column was equilibrated with 20% ACN, 0.1% TFA. A linear gradient of ACN and water, both containing 0.1% TFA, was used from 20 to 50% ACN in 60 min with a flow rate of 1 ml/min (0.5%/min). Obtained proteins were lyophilized and resolved in water. Correct masses were verified by electrospray mass spectrometry. Peptide concentrations were measured in water using absorbance at 280 nm and peptide specific extinction coefficients.

Circular Dichroism Spectroscopy

CD measurements were carried out with a temperature-controlled Jasco J-810 CD spectrapolarimeter. For all measurements, a path length of 0.5 cm was used. Spectra were obtained with samples containing 4.8 μM of each protein and equimolar amounts of double-stranded E-Box DNA (5′-GTC AGTCAGCCACGTGATCGGTCA-3′, consensus for Myc/Max binding site is underlined) or AP-1 DNA (5′-GTCAGTCAG TGACTCAATCGGTCA-3′ consensus for Jun : Fos binding site is underlined), respectively, in CD buffer (10 mM potassium phosphate, 100 mM KF, pH 7). The spectra represent an average of three scans. Temperature denaturation profiles were recorded at 222 nm from −8 to 85 °C, with a temperature gradient of 0.6 °C/min. All profiles were found to be reversible. Apparent T_m values were determined by least-squares curve fitting of equilibrium denaturation curves [38–41] assuming a two-state model of a folded peptide dimer unfolding to a monomer, a model which is well-established and valid for most coiled coils [24,34,42,43]. ΔT_m of a heterodimer AB was calculated by using $\Delta T_m(AB) = T_m(AB) - 0.5 \times (T_m(A) + T_m(B))$. Thermal T_m data were converted to generate K_D values from fraction folded and unfolded as reported previously [39].

Gel Shift Assay

Purified bMyc, bMax, aMax and aMip proteins were mixed in various ratios and added to either E-Box DNA, or AP-1 DNA as negative control. DNA was labeled with ^{32}P-γ-ATP and diluted to 5000 Cherenkov counts/μl. Purified proteins were incubated for 30 min on ice in reaction buffer (1 × buffered saline (BS), 25 ng/μl poly(dI-dC), 5 mM DTT, 0.06% NP40, 0.625 μg/μl BSA; with 2 × BS buffer: 20 mM Hepes, pH 7.9, 120 mM KCl, 8% ficoll, 2 mM EDTA, 10 mM $MgCl_2$) and 1 μl labeled DNA. The binding complexes were resolved on a native 6% polyacrylamide gel in 0.5× tris-borate-EDTA (TBE) buffer (taken from a 10x stock solution: 1 M Tris, 1 M boric acid, 25 mM EDTA) and visualized by autoradiography from dried gels. Densitometric quantification of gel bands was performed using ImageJ software [44]. The ratio between the signal of the shifted band to the added signals of all bands within each lane was calculated from integrated peaks. Percent signal intensity was determined relative to the averaged values from the lanes of the Myc : Max : DNA without inhibitor.

RESULTS

Library Design, Selection of Mip and Generation of Human aMax

To identify peptides binding to the c-Myc coiled coil region, we varied the *a*, *d*, *e*, and *g* positions (Figure 1) as these positions are at the Myc : Max interface and predicted to be important for interaction specificity and stability. Outer (*b*, *c*, and *f*) positions were identical to human Max with two exceptions, position *f*1 of the library was changed to E to introduce the N-cap motif (S-X-X-E) [45,46], and Y was inserted at the *c*2 position of wt Max and the library, and at the *f*2 position of Myc for protein concentration determination.

The core residues of coiled coils (positions *a* and *d*) have an impact on specificity, stability and oligomerization state. It was observed that in dimeric Zip's, the β-branched hydrophobic residues I and V are favored at *a* positions whereas γ-branched L is highly favored at *d* positions because of sterical reasons [21]. With the exception of Myc position *d*1 and Max position *d*1 and *d*2, all *d* positions are L. Consequently, we

DOI: 10.1002/psc

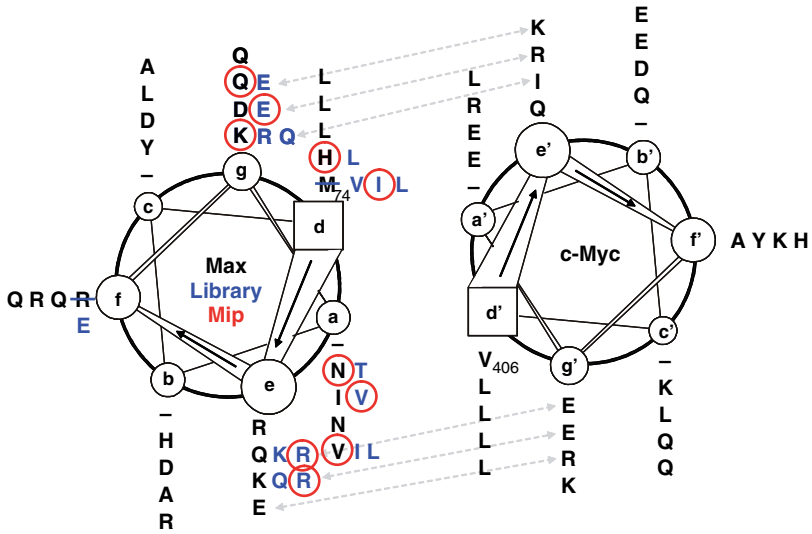

Figure 1 Helical wheel projection of the Myc : Max leucine zipper, the library and the selected Mip sequence, looking down the helix axis from the *N*- to the *C*-terminus. Wild-type amino acids of the Myc and Max leucine zipper region are given in black. Additional residues implemented in the library are indicated in blue, wild-type residues removed from libraries are struck through in blue, and residues selected in Mip are circled red. Peptides start with position *d*, hence, there is no *a*, *b*, and *c* position in the first heptad (indicated with –). Position *f*1 of the library was changed to E for additional N-cap stability; position *c*2 in Max and the library, as well as position *f*2 in Myc, were changed to Y to assist with concentration determination.

included L in positions *d*1 and *d*2 in the library. Wt M at *d*1 of Max was excluded from the library because of lower helical propensity and to avoid oxidation [47,48]. Instead, a choice of L, V, I was provided. Position *d*2 retained wt H in addition to library option L.

The *a* position is more tolerant to changes in amino acids than the *d* position [49]. Preferences for amino acids at position *a* were difficult to predict as three of the four *a* positions of Myc are occupied by charged amino acids: E at position *a*2 and *a*3, and R at *a*4. Therefore, we retained the wt Max residues and included further options. At position *a*5, options I and L were added to wt V, the most commonly occurring and stabilizing amino acids in position *a*. At position *a*3, only β-branched I and V were included into the library to keep the library size manageable. The Myc derivative Omomyc by Soucek *et al.*, interacts better with Myc than with Max because of T in position *a*2, I in *a*3, N in *a*4, and Q in *g*3 [50]. Consequently, we included all of these residue options in our library. N_{a4} was kept constant as it is structurally important for the interaction stability and specificity in the Myc : Max heterodimer [28,50].

Positions *e* and *g*, flanking the hydrophobic core, can increase coiled coil stability and specificity by forming ionic interactions with *g*′ and *e*′ positions of the other helix. A thermodynamic scale for residues at *e* and *g* positions has been reported [51]. Krylov and colleagues ranked stabilities of *e*–*g* pairs as follows: E–R > E–K > Q–Q > R–Q ≥ K–Q > Q–E > K–K > R–R ≥ K–R > E–E. As Myc *g*1 and *g*2 are occupied with E, we offered K, R and Q in opposing *e* positions (*e*2, *e*3) in the library. Position *e*4 E was not varied as its interaction with R_{g3} in Myc seemed to be already optimal. The preference for library position *g*1 opposing I at *e*2 in Myc is difficult to predict. We, therefore, chose amino acids with some hydrophobic character (K, R, Q) which are also commonly found at *e* and *g* positions. For positions *g*2 D and *g*3 Q, opposing R_{e3} or K_{e4} in Myc, wt residues were kept and E was added to permit complementary ion pairs.

A PCA [24,34,35] was used to select for peptides binding the Myc coiled coil. For this assay, library members were genetically fused to one half of the murine enzyme mDHFR, and Myc was linked to the other half. Only interaction between Myc and a library member renders the enzyme active and leads to colonies under selective conditions. Best performing clones were enriched by growth competition under selective conditions. As it has been reported for this PCA-assay, stochastical selection can be excluded [35]. Sequencing after ten growth passages identified one predominant sequence, termed Mip. Mip differed in five of the ten randomized positions from the wt Max sequence (Figure 1); positions *d*2, *a*1, *a*4, *g*1, and *g*3, retained wt Max residues. Importantly, the positions were selected at a different rate (Table 1). At the *d*1 position, the only position, where the wt Max residue was not included, I was favored over V after only two rounds of growth competition. At position *a*3, V was selected over wt I after round five. In the core flanking *e* and *g* positions, R was selected twice over Q (position *e*2) and K (position *e*3) after round two. Selection at position *g*2 for E instead of D occurred in selection round four. Retained wt residues were selected late in round four (Q_{g3}), round six (K_{g1} and V_{a5}), and round eight (N_{a2} and H_{d2}).

DOI: 10.1002/psc

Table 1 Selected residues in pool sequences after various rounds of growth competition

Heptad	*d*1	*g*1	*a*2	*d*2	*e*2	*g*2	*a*3	*e*3	*g*3	*a*5
Max[a]	M	K	N	H	Q	D	I	K	Q	V
Library[b]	L/V/I	K/R/Q	T/N	H/L	K/R/Q	E/D	V/I	K/R/Q	E/Q	L/V/I
P1	L/V[c]	K/R/Q	N/T	L(H)[d]	R(K/Q)	D/E	I/V	K/R/Q	Q/E	V(L/I)
P2	I	R	T	L(H)	R	D	I(V)	R	Q(E)	V/I(L)
P4	I	R(K/Q)	N/T	H(L)	R	E	V(I)	R	Q	I(V)
P5	I	K/R/Q	N(T)	H(L)	R	E	V	R	Q	V/I
P6	I	K	N(T)	H(L)	R	E	V	R	Q	V
P8	I	K	N	H	R	E	V	R	Q	V
P10	I	K	N	H	R	E	V	R	Q	V

[a] Max sequence: MRRKNHYHQQDIDDLKRQNALLEQQVRAL.
[b] Library sequence:(*d*1)RE(*g*1) (*a*2)HY(*d*2)(*e*2)Q(*g*2) (*a*3)DDL(*e*3)R(*g*3) NALLEQQ (*a*5)RAL.
[c] X/Y indicates approximately equal distribution of amino acid X and Y.
[d] X(Y) indicates a predominance of amino acid X over Y.

To generate potent inhibitors able to interfere with the DNA-bound state of Myc : Max, we used an acidic extension, which had been designed for the mouse homologues [36]. We fused this acidic extension to the human wt Max HLHZip region (denoted aMax) as well as to the PCA-selected Mip (denoted aMip) and tested the stability with Myc and the ability to interfere with Myc : Max or Myc : Max : DNA complexes.

Thermal Stability of Mip, Myc and Max Complexes

Secondary structure, as well as thermal unfolding of various combinations of Myc, Max, and Mip peptides, was monitored by CD spectroscopy. Consistent with published data, the Myc and Max Zip domains alone were very unstable (data not shown). Consequently, we extended the Myc and Max Zip peptides with the human basic DNA-binding region and the human HLH motif (denoted bMyc, bMax).

The CD spectra of the corresponding peptides alone or in various combinations were recorded in the presence and absence of DNA (Figure 2(A) and (B)). All peptides were found to be α-helical, and the ratio of the ellipticity at 222 nm to the ellipticity at 208 nm was found to be greater than 1.0 (Table 2), indicative of coiled coil formation [52]. Among the homodimers, aMip was more helical than bMax and aMax. Among the heterodimers, bMax : aMip displayed the highest helicity, followed by bMyc : aMip, bMax : aMax, bMyc : aMax. The wt bMyc : bMax interaction showed the least helix content. Upon addition of DNA, containing the E-Box binding site (CACGTG), the helicity of the heterodimeric bMyc : bMax complex increased significantly, whereas there was no change for the bMyc : aMip heterodimer (when subtracting the DNA spectrum). The helicity of bMyc : aMip with or without DNA was still higher than that of bMyc : bMax with DNA.

Table 2 Thermodynamic data of various complexes of bMyc, bMax, aMip and aMax in the absence or presence of E-Box DNA

	T_m [°C]	K_D(37 °C) [μM]	ΔG(37 °C) [kcal/mol]	$\theta_{222}/\theta_{208}$[a]
Homodimers:				
bMyc[b]	—	—	—	—
bMax	32	33 000	6.4	1.03
aMax	47	98	9.9	1.11
aMip	47	130	9.8	1.08
Heterodimers:				
bMyc : bMax	33	30 000	6.4	1.05
bMyc : aMip	46	250	9.4	1.03
bMax : aMip	47	61	10.2	1.09
bMyc : aMax	48	460	8.5	1.12
bMax : aMax	46	3400	7.8	0.91
+E-Box DNA:				
bMyc : bMax : E-box	49	11	11.3	1.54
bMyc : aMip : E-box	46	180	9.6	1.13

[a] Results of CD spectra at 20 °C.
[b] The T_m, K_D, and ΔG of bMyc could not be determined due to its low stability.

Thermal denaturation curves were obtained over a temperature range of −8 to 85 °C (Figure 2(C) and (D)), and T_m values were calculated assuming a two-state transition of folded dimer to unfolded monomers (Table 2). Importantly, the calculated average of the corresponding homodimer curves is lower than the curve of the mixture, indicating heterotypic interaction. For bMyc, no T_m value could be determined because of its instability. Next to bMyc, bMax exhibited the lowest stability with a T_m of 32 °C. Importantly, the T_m of bMyc : aMip ($T_m = 46$ °C) is 13 °C higher compared to bMyc : bMax ($T_m = 33$ °C), and in the same range as bMyc : bMax : DNA ($T_m = 49$ °C). As expected, DNA

DOI: 10.1002/psc

addition had no significant effect on the stability of the bMyc : aMip complex. Also bMax : aMip ($T_m = 47\,^{\circ}C$) showed comparable stability to bMyc : bMax : DNA and should then be able to compete with DNA binding. The T_m values of all heterodimeric complexes with aMax are between 46 and 48 °C, and hence similar to the bMyc : aMip interaction.

Inhibition of Myc : Max : DNA Complexes

Gelshift assays (Figures 3 and 4) were performed to investigate DNA binding of bMyc : bMax or bMax : bMax complexes in the presence or absence of the inhibitors aMip and aMax. bMax homodimers and bMyc : bMax heterodimers, but not bMyc homodimers, should be

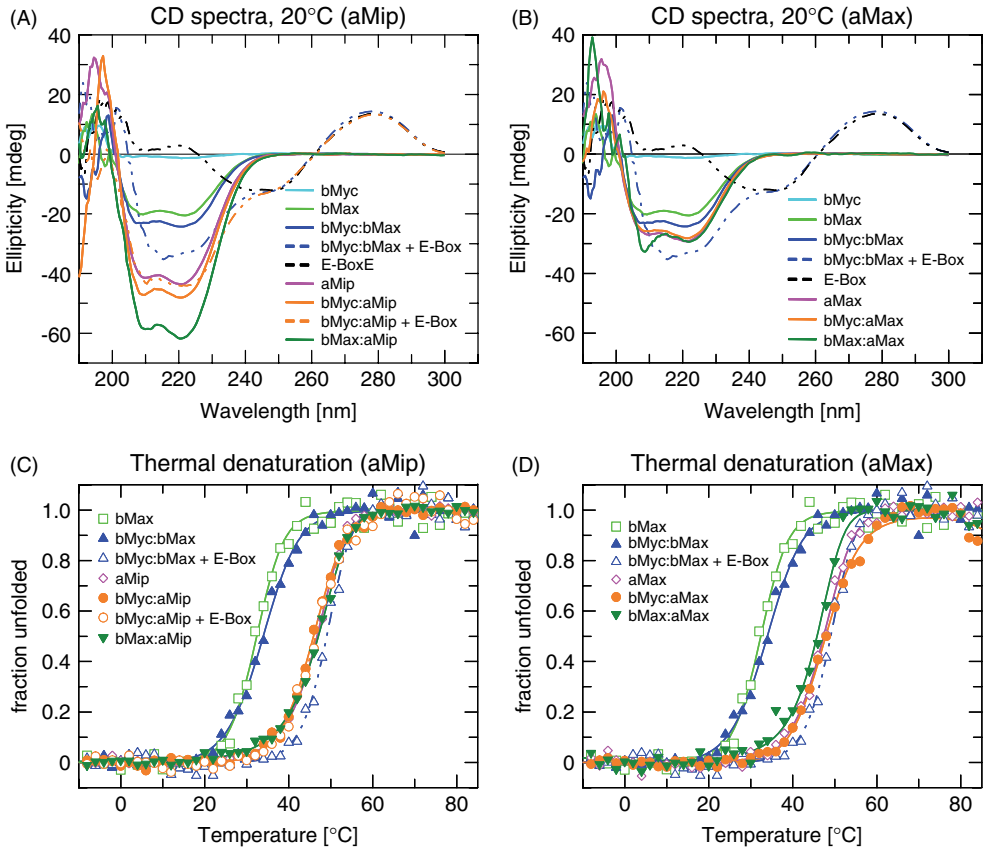

Figure 2 Biophysical characterization of possible homo- and heterodimers. CD spectra at 20 °C of all possible homo- and heterodimer combinations with aMip (A) and aMax (B). Thermal denaturation curves of all possible homo- and heterodimer combinations with aMip (C) and aMax (D). Spectra and melts including E-Box DNA are indicated by dashed lines.

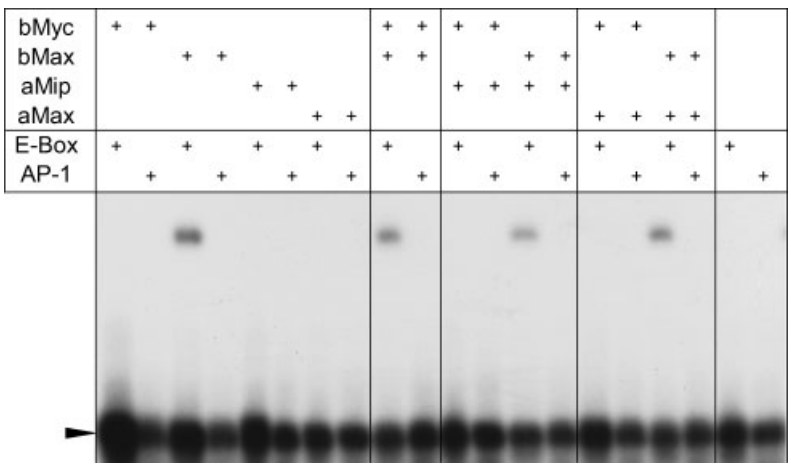

Figure 3 Gel shift of homo- and heterodimers with DNA containing either E-Box or AP-1 binding sites. Each lane contains 50 ng/µl of homodimers or 100 ng/µl of heterodimers (50 ng/µl of each protein). The arrowhead indicates free DNA.

DOI: 10.1002/psc

able to bind DNA, containing the E-Box sequence CACGTG.

To analyze the binding specificities of the different constructs, the binding of all homo- and heterotypic complexes was tested with the E-Box DNA and the AP-1-specific sequence TGACTCA as negative control (Figure 3) [53]. Reassuringly, none of the probes tested bound to the AP-1 recognition sequence. As expected, bMax as well as bMyc : bMax, but not bMyc, showed a gel shift with E-Box DNA. Additionally, bMax : aMip and bMax : aMax displayed a gel shift, possibly due to bMax homodimers binding to the E-Box DNA. In contrast, no DNA binding was detected for bMyc : aMip or bMyc : aMax.

In order to characterize the ability of aMip and aMax to interfere with DNA binding of bMyc : bMax heterodimers, increasing amounts of aMip or aMax, respectively, were added to the respective complex (Figure 4). Both inhibitors abolished the DNA binding of bMyc : bMax in a concentration-dependent manner. Densitometric quantification of the bands revealed a similar inhibition pattern for both inhibitors (Figure 4, bottom panel). In agreement with the thermodynamic stabilities, an equimolar ratio resulted in about 50% inhibition.

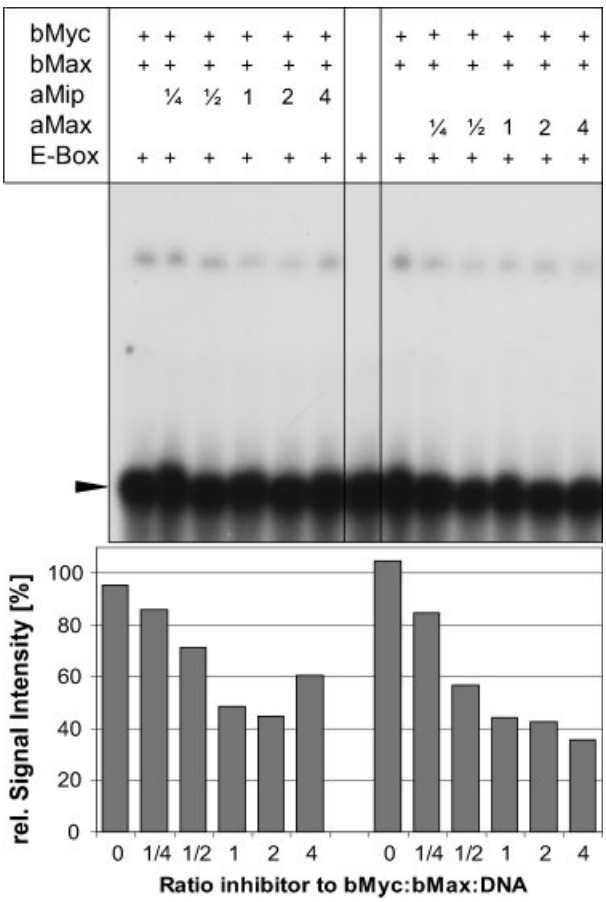

Figure 4 Competitive gel shift assay and results of densitometric analysis. Increasing molar equivalents of aMip and aMax (25 to 400 ng/μl) were added to bMyc : bMax (50 ng/μl of each protein) together with E-Box DNA. The arrowhead indicates free DNA. The total concentration of bMyc : bMax is 100 ng/μl. Numbers for aMip and aMax represent their molar ratio to the total concentration of bMyc : bMax.

DISCUSSION

The aim of this study was to inhibit the Myc : Max : DNA interaction with interfering peptides. Two approaches were chosen, a dominant-negative Max sequence (aMax) and a peptide selected from a genetic library (aMip). The enriched sequence differed in five out of ten randomized positions from the Max sequence. The library design was mainly based on maximizing charge attractions, while minimizing repulsion and steric hindrance. Data from structural studies [28,30,31], as well as other designs [50], were also considered.

Generally, position *d* is occupied by L. Surprisingly, in both cases other options were selected. In position *d*1, I was selected already in round two over L and V for reasons which are not easy to rationalize. Possibly, I packs better in this context with V_{d1} of Myc and might accommodate the atypical *a* layer (N–E) better. In position *d*2, wt H from the Max sequence remained. Although it dominated early in the selection procedure (round four), it was clearly selected only after round eight. This suggests that both options are acceptable choices at this position. Structural analysis showed that the E residues in *a*1 and *a*2 of Myc form ion pairs with H_{d2} of Max and are responsible for heterodimerization specificity [30], which might explain the slight preference for H. According to Tchan *et al.* [54] H_{d2} also destabilizes the Max homodimer, thereby increasing its interaction preference for Myc.

Residue preferences at *a* positions are difficult to rationalize because of the charged Myc core. In two of the three positions, wt Max sequences were retained. Interestingly, none of the options taken from Omomyc [50] was selected. According to their results, T in position *a*2 and I in position *a*3 provide better shape complementarity with core residues in Myc. However, in our selection wt N_{a2} was retained and V was selected at *a*3. As N_{a2} was selected only in round eight of the growth competition, with a slight dominance only from round five on, it is likely that both residue options confer comparable stability to the complex. Myc's *a* positions have three out of four charged residues, and pairing preferences for a–a′ pairs have mostly been tested with hydrophobic amino acids as well as K, and N [55]. Only recently, a more comprehensive study reported values for residues R and E also [56]. According to this study, E has a lower coupling energy pairing with T compared to N, and with V compared to I. This could explain why V was preferred over I but it fails to explain the slight preference for a N–E pair at *a*2.

DOI: 10.1002/psc

According to Krylov and colleagues, E–R is the most stable interhelical pair in *e* and *g* positions [51]. Consistent with these results, at all three possible positions E–R pairs were selected. Furthermore, enrichment at these three positions occurred early in the selection process indicative of the importance of these interactions: R_{e2} and R_{e3}, facing E_{g1} and E_{g2} in Myc, were selected already after two passages of growth competition, and E_{g2}, opposing R_{e3} in Myc, was selected after four rounds. A similarly fast enrichment of E–R pairs has been reported previously [24,41]. Surprisingly, for *g*3, opposing K_{e4} in Myc, wt Q was retained instead of selecting E. However, according to Krylov *et al.*, the energetic difference between an E–K and Q–K pair is only −0.15 kcal/mol [51]. Additionally, the Omomyc design also used Q at this position [50]. Furthermore, in the crystal structure, the tetrad Myc R_{g3} and R_{a3}, together with Max Q_{g3} and N_{a3} was found to have a tighter intermolecular packing than the corresponding tetrad in the Max homodimer, resulting in a preference for the heterodimer [28]. This could explain the positional preference of Q over K at this position. Residue K_{g1} faces I_{e2} in Myc, a hydrophobic residue which is not common for *e* or *g* positions. In some coiled coils, it was observed that buried, polar residues in *a*′ position interact also with complementary residues at *g* positions [57,58]. Myc *a*2 is occupied by negatively charged E and could possibly interact with K_{g1} explaining a preference of K over Q. Discrimination between K and R could be for steric reasons. Among all varied *e* and *g* positions, this position was selected last at round six, however, a preference for positive charged residues is seen early in the selection process.

Randomized positions that settled very early during the growth competition possibly have a larger contribution to the dimer stability as amino acids that came up later. Hence, the selection of I_{d1}, R_{e2}, and R_{e3} in round two should play a predominant role for dimer stability compared to other randomized positions. Interestingly, four out of five *e* and *g* positions, but only one out of five *a* and *d* positions, were selected early before round five. Positions selected early coincide with residue interactions known to be stabilizing and typically found in coiled coils sequences. In contrast, positions selected at a slower rate were almost always occupied by less common residues. The slow selection rate is most likely due to nonoptimal residue compatibility resulting in more than one energetically similar solution. In addition, *in vivo* factors, such as higher stability in *E. coli* or better expression, certainly also played a role in the Mip selection. Such factors are difficult to rationalize at the sequence level, emphasizing the importance of a combinatorial approach.

Structural integrity and stability of the respective peptides were measured by CD spectra and denaturation curves. The Zip domain on its own was not stable enough to obtain meaningful data. In published results, Myc and Max Zip's had been disulfide-bridged [30,31], measurements had been conducted under various conditions (pH, ionic strength, etc.) [29,59], or the murine [36], viral or chicken bHLHZip homologs [60] had been used to increase stability. However, for *in vivo* applications, the target sequence must remain unchanged, and additionally, stabilization by DNA binding needs to be taken into account. Hence, we measured stabilities of the full bHLHZip domain instead of only the Zip domain. Using murine sequences, it was shown that the substitution of the basic region of Max with an acidic extension sequestered the basic region of Myc and thus abolished DNA binding of the bHLHZip complex of Myc : Max [36]. Similarly, we tested this strategy for Mip as well as for the human Max sequence.

The observed higher helix content of our acidic extended heterodimers compared to bMax : bMyc (Figure 2) is in agreement with results obtained with murine sequences, where it was proposed that the acidic extension adopts a helical structure when paired with the basic region [36]. Compared to data from murine sequences [36], complexes with human bMyc are generally less stable (bMyc : bMax and bMyc : aMax) with a T_m difference of 16 to 18 °C, whereas almost no difference between human and murine bMax and aMax, alone or in combination, can be detected under similar experimental conditions. These findings can be attributed to several factors: The murine Myc and Max bHLHZip regions differ not only in sequence but also in length from the human versions. The murine Myc sequence is five, and the murine Max sequence is 11 residues longer. Within the overlapping parts, murine and human Max have only one amino acid difference located at position *b*2 (D vs H) of the coiled coil. However, murine and human Myc vary in six residues. Among these, four are within the Zip, occupying positions *d*1 (I vs V), *g*1 (D vs E), *b*2 (H vs Q), and *a*3 (K vs E), with the last one even oppositely charged, allowing for beneficial interactions of K_{a3} in murine Myc with D_{g2} in Max. These differences explain why complexes with murine Myc are considerably more stable than those with human Myc, whereas no significant differences were found for complexes with murine or human Max.

Electrophoretic mobility shift assays (EMSA) demonstrated that binding was specific for E-box DNA, and from the various combinations probed, only bMyc : bMax heterodimers and bMax homodimers bound E-box DNA as expected. The ability of the selected aMip and aMax to not only interfere with Myc : Max dimerization but also prevent the DNA binding of the Myc : Max bHLHZip complex was demonstrated with a competitive gel shift assay. About 50% inhibition of the DNA-bound complex was already achieved with an equimolar mixture. A direct comparison to the previously reported Myc-derived Omomyc, which forms dimers with Myc and Max [50], is difficult as that study used GST-tagged peptides as well as

DOI: 10.1002/psc

5-fold excess of Myc and 5- to 20-fold excess of Omomyc relative to Max. However, only a slight decrease of the band intensity of Myc : Max : DNA complex is visible in the presence of excess Omomyc, suggesting that aMip and aMax are more potent inhibitors.

In summary, we developed two sequences, aMax and aMip which bind bMyc with considerably higher stability than wild-type bMax. Thus, both inhibitors were able to successfully compete with the DNA-bound stage of bMyc and bMax. The inhibitory effect of aMax and aMip on Myc : Max activity will make them useful research tools for the analysis of Myc action in physiological and oncogenic circumstances. Furthermore, they might serve as lead compounds for the development of Myc-specific drugs.

Acknowledgements

We like to thank Catherine Chen, Hannah Rabenstein and Neele Hübner for their help with experiments, and Jody Mason for proof-reading the manuscript. This work was funded in the Emmy Noether program of the Deutsche Forschungsgemeinschaft (grant Ar 373/1-1, 1-2).

REFERENCES

1. Pelengaris S, Khan M, Evan G. c-MYC: more than just a matter of life and death. *Nat. Rev. Cancer* 2002; **2**: 764–776.
2. Nesbit CE, Tersak JM, Prochownik EV. MYC oncogenes and human neoplastic disease. *Oncogene* 1999; **18**: 3004–3016.
3. Jain M, Arvanitis C, Chu K, Dewey W, Leonhardt E, Trinh M, Sundberg CD, Bishop JM, Felsher DW. Sustained loss of a neoplastic phenotype by brief inactivation of MYC. *Science* 2002; **297**: 102–104.
4. Felsher DW, Bishop JM. Reversible tumorigenesis by MYC in hematopoietic lineages. *Mol. Cell.* 1999; **4**: 199–207.
5. Felsher DW. Reversibility of oncogene-induced cancer. *Curr. Opin. Genet. Dev.* 2004; **14**: 37–42.
6. Boxer RB, Jang JW, Sintasath L, Chodosh LA. Lack of sustained regression of c-MYC-induced mammary adenocarcinomas following brief or prolonged MYC inactivation. *Cancer Cell* 2004; **6**: 577–586.
7. Shachaf CM, Felsher DW. Tumor dormancy and MYC inactivation: pushing cancer to the brink of normalcy. *Cancer Res.* 2005; **65**: 4471–4474.
8. Shachaf CM, Kopelman AM, Arvanitis C, Karlsson A, Beer S, Mandl S, Bachmann MH, Borowsky AD, Ruebner B, Cardiff RD, Yang Q, Bishop JM, Contag CH, Felsher DW. MYC inactivation uncovers pluripotent differentiation and tumour dormancy in hepatocellular cancer. *Nature* 2004; **431**: 1112–1117.
9. D'Agnano I, Valentini A, Gatti G, Chersi A, Felsani A. Oligopeptides impairing the Myc-Max heterodimerization inhibit lung cancer cell proliferation by reducing Myc transcriptional activity. *J. Cell. Physiol.* 2007; **210**: 72–80.
10. Berg T, Cohen SB, Desharnais J, Sonderegger C, Maslyar DJ, Goldberg J, Boger DL, Vogt PK. Small-molecule antagonists of Myc/Max dimerization inhibit Myc-induced transformation of chicken embryo fibroblasts. *Proc. Natl. Acad. Sci. U.S.A.* 2002; **99**: 3830–3835.
11. Kiessling A, Sperl B, Hollis A, Eick D, Berg T. Selective inhibition of c-Myc/Max dimerization and DNA binding by small molecules. *Chem. Biol.* 2006; **13**: 745–751.
12. Vennstrom B, Sheiness D, Zabielski J, Bishop JM. Isolation and characterization of c-myc, a cellular homolog of the oncogene (v-myc) of avian myelocytomatosis virus strain 29. *J. Virol.* 1982; **42**: 773–779.
13. Hurlin PJ, Huang J. The MAX-interacting transcription factor network. *Semin. Cancer Biol.* 2006; **16**: 265–274.
14. Littlewood TD, Evan GI. Transcription factors 2: helix-loop-helix. *Protein Profile* 1995; **2**: 621–702.
15. Marchetti A, Abril-Marti M, Illi B, Cesareni G, Nasi S. Analysis of the Myc and Max interaction specificity with lambda repressor-HLH domain fusions. *J. Mol. Biol.* 1995; **248**: 541–550.
16. Woolfson DN. The design of coiled-coil structures and assemblies. *Adv. Protein Chem.* 2005; **70**: 79–112.
17. Lupas AN, Gruber M. The structure of alpha-helical coiled coils. *Adv. Protein Chem.* 2005; **70**: 37–78.
18. Mason JM, Arndt KM. Coiled coil domains: stability, specificity, and biological implications. *ChemBioChem* 2004; **5**: 170–176.
19. Mason JM, Müller KM, Arndt KM. Considerations in the design and optimization of coiled coil structures. *Methods Mol. Biol.* 2007; **352**: 35–70.
20. Wolf E, Kim PS, Berger B. MultiCoil: a program for predicting two- and three-stranded coiled coils. *Protein Sci.* 1997; **6**: 1179–1189.
21. Harbury PB, Zhang T, Kim PS, Alber T. A switch between two-, three-, and four-stranded coiled coils in GCN4 leucine zipper mutants. *Science* 1993; **262**: 1401–1407.
22. O'Shea EK, Lumb KJ, Kim PS. Peptide 'Velcro': Design of a heterodimeric coiled coil. *Curr. Biol.* 1993; **3**: 658–667.
23. Hu JC, Newell NE, Tidor B, Sauer RT. Probing the roles of residues at the e and g positions of the GCN4 leucine zipper by combinatorial mutagenesis. *Protein Sci.* 1993; **2**: 1072–1084.
24. Arndt KM, Pelletier JN, Müller KM, Plückthun A, Alber T. Comparison of in vivo selection and rational design of heterodimeric coiled coils. *Structure (Camb)* 2002; **10**: 1235–1248.
25. Grandori C, Cowley SM, James LP, Eisenman RN. The Myc/Max/Mad network and the transcriptional control of cell behavior. *Annu. Rev. Cell Dev. Biol.* 2000; **16**: 653–699.
26. Ayer DE, Eisenman RN. A switch from Myc : Max to Mad : Max heterocomplexes accompanies monocyte/macrophage differentiation. *Genes Dev.* 1993; **7**: 2110–2119.
27. Amati B, Brooks MW, Levy N, Littlewood TD, Evan GI, Land H. Oncogenic activity of the c-Myc protein requires dimerization with Max. *Cell* 1993; **72**: 233–245.
28. Nair SK, Burley SK. X-ray structures of Myc-Max and Mad-Max recognizing DNA. Molecular bases of regulation by proto-oncogenic transcription factors. *Cell* 2003; **112**: 193–205.
29. Muhle-Goll C, Gibson T, Schuck P, Schubert D, Nalis D, Nilges M, Pastore A. The dimerization stability of the HLH-LZ transcription protein family is modulated by the leucine zippers: a CD and NMR study of TFEB and c-Myc. *Biochemistry* 1994; **33**: 11296–11306.
30. Lavigne P, Kondejewski LH, Houston ME Jr, Sonnichsen FD, Lix B, Skyes BD, Hodges RS, Kay CM. Preferential heterodimeric parallel coiled-coil formation by synthetic Max and c-Myc leucine zippers: a description of putative electrostatic interactions responsible for the specificity of heterodimerization. *J. Mol. Biol.* 1995; **254**: 505–520.
31. Lavigne P, Crump MP, Gagne SM, Hodges RS, Kay CM, Sykes BD. Insights into the mechanism of heterodimerization from the 1H-NMR solution structure of the c-Myc-Max heterodimeric leucine zipper. *J. Mol. Biol.* 1998; **281**: 165–181.
32. Blackwood EM, Eisenman RN. Max: a helix-loop-helix zipper protein that forms a sequence-specific DNA-binding complex with Myc. *Science* 1991; **251**: 1211–1217.
33. Koskinen PJ, Ayer DE, Eisenman RN. Repression of Myc-Ras cotransformation by Mad is mediated by multiple protein-protein interactions. *Cell Growth Differ.* 1995; **6**: 623–629.
34. Arndt KM, Pelletier JN, Müller KM, Alber T, Michnick SW, Plückthun A. A heterodimeric coiled-coil peptide pair selected in vivo from a designed library-versus-library ensemble. *J. Mol. Biol.* 2000; **295**: 627–639.

35. Pelletier JN, Arndt KM, Plückthun A, Michnick SW. An in vivo library-versus-library selection of optimized protein-protein interactions. *Nat. Biotechnol.* 1999; **17**: 683–690.
36. Krylov D, Kasai K, Echlin DR, Taparowsky EJ, Arnheiter H, Vinson C. A general method to design dominant negatives to B-HLHZip proteins that abolish DNA binding. *Proc. Natl. Acad. Sci. U.S.A.* 1997; **94**: 12274–12279.
37. Pelletier JN, Campbell-Valois FX, Michnick SW. Oligomerization domain-directed reassembly of active dihydrofolate reductase from rationally designed fragments. *Proc. Natl. Acad. Sci. U.S.A.* 1998; **95**: 12141–12146.
38. Becktel WJ, Schellman JA. Protein stability curves. *Biopolymers* 1987; **26**: 1859–1877.
39. Mason JM, Müller KM, Arndt KM. Positive aspects of negative design: simultaneous selection of specificity and interaction stability. *Biochemistry* 2007; **46**: 4804–4814.
40. Mason JM, Hagemann UB, Arndt KM. Improved stability of the Jun-Fos Activator Protein-1 coiled coil motif: a stopped-flow circular dichroism kinetic analysis. *J. Biol. Chem.* 2007; **282**: 23015–23024.
41. Mason JM, Schmitz MA, Müller KM, Arndt KM. Semirational design of Jun-Fos coiled coils with increased affinity: Universal implications for leucine zipper prediction and design. *Proc. Natl. Acad. Sci. U.S.A.* 2006; **103**: 8989–8994.
42. O'Shea EK, Rutkowski R, Kim PS. Mechanism of specificity in the Fos-Jun oncoprotein heterodimer. *Cell* 1992; **68**: 699–708.
43. Krylov D, Mikhailenko I, Vinson C. A thermodynamic scale for leucine zipper stability and dimerization specificity: e and g interhelical interactions. *EMBO J.* 1994; **13**: 2849–2861.
44. Abramoff MD, Magelhaes PJ, Ram SJ. Image processing with Image. *J. Biophoton. Int.* 2004; **11**: 36–42.
45. Peterson RW, Nicholson EM, Thapar R, Klevit RE, Scholtz JM. Increased helix and protein stability through the introduction of a new tertiary hydrogen bond. *J. Mol. Biol.* 1999; **286**: 1609–1619.
46. Lu M, Shu W, Ji H, Spek E, Wang L, Kallenbach NR. Helix capping in the GCN4 leucine zipper. *J. Mol. Biol.* 1999; **288**: 743–752.
47. Gromiha MM, Parry DA. Characteristic features of amino acid residues in coiled-coil protein structures. *Biophys. Chem.* 2004; **111**: 95–103.
48. O'Neil KT, DeGrado WF. A thermodynamic scale for the helix-forming tendencies of the commonly occurring amino acids. *Science* 1990; **250**: 646–651.
49. Hu JC, O'Shea EK, Kim PS, Sauer RT. Sequence requirements for coiled-coils: analysis with lambda repressor-GCN4 leucine zipper fusions. *Science* 1990; **250**: 1400–1403.
50. Soucek L, Helmer-Citterich M, Sacco A, Jucker R, Cesareni G, Nasi S. Design and properties of a Myc derivative that efficiently homodimerizes. *Oncogene* 1998; **17**: 2463–2472.
51. Krylov D, Barchi J, Vinson C. Inter-helical interactions in the leucine zipper coiled coil dimer: pH and salt dependence of coupling energy between charged amino acids. *J. Mol. Biol.* 1998; **279**: 959–972.
52. Monera OD, Zhou NE, Kay CM, Hodges RS. Comparison of antiparallel and parallel two-stranded alpha-helical coiled-coils. Design, synthesis, and characterization. *J. Biol. Chem.* 1993; **268**: 19218–19227.
53. Eferl R, Wagner EF. AP-1: a double-edged sword in tumorigenesis. *Nat. Rev. Cancer* 2003; **3**: 859–868.
54. Tchan MC, Weiss AS. Asn(78) and His(81) form a destabilizing locus within the Max HLH-LZ homodimer. *FEBS Lett.* 2001; **509**: 177–180.
55. Acharya A, Ruvinov SB, Gal J, Moll JR, Vinson C. A heterodimerizing leucine zipper coiled coil system for examining the specificity of a position interactions: amino acids I, V, L, N, A, and K. *Biochemistry* 2002; **41**: 14122–14131.
56. Acharya A, Rishi V, Vinson C. Stability of 100 homo and heterotypic coiled-coil a-a′ pairs for ten amino acids (A, L, I, V, N, K, S, T, E, and R). *Biochemistry* 2006; **45**: 11324–11332.
57. Havranek JJ, Harbury PB. Automated design of specificity in molecular recognition. *Nat. Struct. Biol.* 2003; **10**: 45–52.
58. Campbell KM, Lumb KJ. Complementation of buried lysine and surface polar residues in a designed heterodimeric coiled coil. *Biochemistry* 2002; **41**: 7169–7175.
59. Muhle-Goll C, Nilges M, Pastore A. The leucine zippers of the HLH-LZ proteins Max and c-Myc preferentially form heterodimers. *Biochemistry* 1995; **34**: 13554–13564.
60. Fieber W, Schneider ML, Matt T, Krautler B, Konrat R, Bister K. Structure, function, and dynamics of the dimerization and DNA-binding domain of oncogenic transcription factor v-Myc. *J. Mol. Biol.* 2001; **307**: 1395–1410.